Journal of Chromatography A, 1283 (2013) 68–74

Contents lists available at SciVerse ScienceDirect

Journal of Chromatography A

journal homepage: www.elsevier.com/locate/chroma

Synthesis of a novel cyclodextrin-derived chiral stationary phase with multiple urea linkages and enantioseparation toward chiral osmabenzene complex

Chun Lin[a], Wenna Liu[a], Jun Fan[a], Yuekui Wang[b,*], Shengrun Zheng[a], Ran Lin[c], Hui Zhang[c,*], Weiguang Zhang[a,*]

[a] Institute of Special Materials, School of Chemistry & Environment, South China Normal University, Guangzhou 510006, China
[b] Institute of Molecular Science, Shanxi University, Taiyuan 030006, China
[c] Department of Chemistry, College of Chemistry and Chemical Engineering, Xiamen University, Xiamen 361005, China

ARTICLE INFO

Article history:
Received 7 November 2012
Received in revised form 21 January 2013
Accepted 22 January 2013
Available online 28 January 2013

Keywords:
Cyclodextrin-based chiral stationary phase
Chiral osmabenzene complex
HPLC enantioseparation
CD spectra
Theoretical calculation

ABSTRACT

A novel chiral stationary phase was synthesized by immobilizing heptakis(6-azido-6-deoxy-2,3-di-*O*-*p*-chlorophenylcarbamoylated)-β-cyclodextrin onto silica gel surface via Staudinger reaction, and applied in enantiomeric separation of a pair of osmabenzene complexes, {Os[CHC(PPh_3)CHC(PPh_3)CH]($C_9H_6NO)_2$}Cl (**1**), which is the first report for enantioseparation of the chiral-only-at-metal osmabenzene complex till now. The effects of separation conditions including salt additives, organic modifiers, pH values, and column temperature on the retention and resolution of the complex have been investigated in detail. Meanwhile, possible chiral recognition mechanism was presented. Chiral complex **1** was well resolved via semi-preparative chiral HPLC technique under optimization conditions and two pure enantiomers were further characterized by analytical HPLC, NMR spectra and solution circular dichroism (CD) spectra, respectively. Furthermore, absolute configuration of the enantiomer was confirmed by theoretical investigation of CD spectra.

1. Introduction

Cyclodextrin-based chiral stationary phases (CSPs) have been widely applied in HPLC enantioseparation of chiral compounds [1,2]. In recent years, many scientists have focused on development of novel linkages between cyclodextrin and silica gels [3–5], and various cyclodextrin-derived chiral selectors [6–8]. In 2002, Ng group reported synthesis of two new chiral stationary phases with multiple urea linkages via Staudinger reaction [9,10], which were derived from perphenylcarbamoylated and permethylated β-cyclodextrin derivatives, respectively. Various chiral analytes were well resolved on two columns under normal or reversed-phase conditions. Compared with traditional CSPs linked by single urea bond [11], these new CSPs exhibited much more stability, due to the cross-linked network-like structure. In addition, two new derived β-cyclodextrin CSPs with multiple triazole linkages were reported in Ng group [12]. These CSPs possessed quite different enantioseparation abilities, compared to the single-"click" derived β-cyclodextrin CSPs [13].

Although there are a variety of applications in resolving chiral organic compounds, enantioseparation of chiral metal complexes on cyclodextrin-based CSPs has been rarely investigated over the past decades [14–16].

Due to both organometallic and aromatic chemical properties, metallabenzene compounds have attracted considerable attention since 1982 [17–20] and showed potential applications in functional materials, such as catalysis, magnetism, and molecular recognition [21]. However, some difficulties in purification and separation via HPLC methods have seriously limited their applications, due to a certain degree of hidden risks to HPLC chiral columns from metal complexes, harsh mobile phase conditions, as well as low separation efficiency. To the best of our knowledge, the related work has not been yet reported to date.

Herein, synthesis of a novel CSP (denoted as MCDP) derived from heptakis(6-azido-6-deoxy-2,3-di-*O*-*p*-chlorophenylcarbamoylated)- β-cyclodextrin and its enantioseparation of a pair of chiral osmabenzene complexes {Os[CHC(PPh_3)CHC (PPh_3)CH]($C_9H_6NO)_2$}Cl (**1**) under polar organic phase will be presented. Separation conditions and mechanism have been investigated in detail. In addition, the absolute configuration of complex **1** was determined by comparison of the calculated circular dichrosim (CD) spectra and the experimental result. This new MCDP exhibits high chemical stabilities as well as selectivity toward osmabenzene complex.

* Corresponding authors. Tel.: +86 20 39310210; fax: +86 20 39310187.
E-mail addresses: ykwang@sxu.edu.cn (Y. Wang), huizhang@xmu.edu.cn (H. Zhang), wgzhang@scnu.edu.cn, fanj@scnu.edu.cn (W. Zhang).

0021-9673/$ – see front matter © 2013 Elsevier B.V. All rights reserved.
http://dx.doi.org/10.1016/j.chroma.2013.01.087

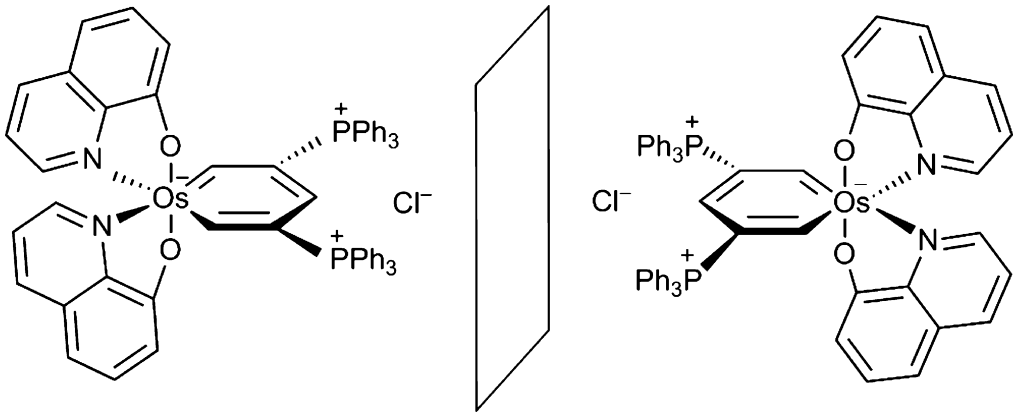

Fig. 1. Molecular structure of a pair of osmabenzene enantiomers (**1**).

2. Experimental

2.1. Chemicals and materials

β-Cyclodextrin was purchased from Shanghai Bio. Life Science and Technology Co., Ltd. (Shanghai, China). Spherical silica gel (5 μm, 100 Å, 300 $m^2\,g^{-1}$) was obtained from Fuji Silysia Chemical Ltd. (Aichi, Japan). Preparation of aminized silica gel was carried out according to the reported method [7]. Osmabenzene complex {Os[CHC(PPh_3)CHC(PPh_3)CH]($C_9H_6NO)_2$}Cl (**1**, Fig. 1) was kindly provided by Professor Xia Hai-ping's group (Xiamen University, China) [20]. Methanol (MeOH), acetonitrile (ACN), n-hexane, 2-propanol (IPA), and ethanol (EtOH) were of HPLC-grade and purchased from LabScience, Inc. (Pittsburg, USA). Ultra-pure water (Aquapro, ARU-L-500L) was used throughout the current research. All other chemicals were of analytical grade and purified prior to use. Stainless steel column tubes were bought from Jiangsu Hanbon Science and Technology Co. Ltd. (China).

2.2. Instruments

Determination of NMR spectra was performed on Varian 400 spectrometer (400 MHz) with tetramethylsilane (TMS) as internal standard at room temperature. IR spectra were recorded with a Perkin-Elmer Spectrum One spectrometer with KBr pellets in the range from 4000 to 400 cm^{-1}. All samples were dried to a constant weight in vacuo at 50 °C for more than 24 h before FT-IR analyses. Elemental analyses were determined on a Perkin-Elmer 2400CHN analyzer. Thermogravimetric analyses (TGA) under air atmosphere were carried out on a Perkin-Elmer TGA7 thermal analyzer with a heating rate of 10 °C min^{-1} from room temperature to 800 °C. Circular dichroism experiments were performed on a JASCO J-815 spectropolarimeter. Evaluation of analytical MCDP column (150 mm × 4.6 mm I.D.) was performed at room temperature, using an HPLC system which consisted of a Shimadzu HPLC system SPD-15C, a Shimadzu UV–vis detector and a 7725i injector equipped with a 20 μL sample loop.

2.3. Synthesis of MCDP

The synthetic route to the desired MCDP is shown in Fig. 2. Compound **I** was prepared as previously reported methods [22,23].

2.3.1. Preparation of heptakis(6-azido-6-deoxy-2,3-di-O-p-chlorophenylcarbamoylated)-β-cyclodextrin (*II*)

p-Chlorophenylisocyanate (12.9 g, 84 mmol) was added into a solution of compound **I** (2.0 g, 1.52 mmol) in anhydrous pyridine (30 mL). The reaction was kept overnight at 90 °C under N_2 atmosphere. After removing pyridine, the resulting residue was extracted with ethyl acetate (100 mL). The combined organic phase was washed with brine, and further dried with anhydrous magnesium sulphate. After being concentrated by half under the reduced pressure, compound **II** was obtained by precipitating with *n*-hexane and filtration [7].

Compound **II**: Yield 76%; m.p.: >200 °C; ^{1}H NMR ($CDCl_3$, TMS, ppm): 8.5–6.7 (m, 70 H); 5.5–3.5 (m, 49 H); FT-IR (KBr pellet, cm^{-1}): 3405 (OH str), 3301 (N—H str), 3072 (C—H str), 2107 (N_3 str), 1722 (C=O str), 1598, 1530, 1492 (arom str), 1054 (sym C—O—C str). Elemental analysis for $C_{140}H_{119}Cl_{14}N_{35}O_{42}$ (3467.87) calcd: C 48.48, H 3.71, N 14.14%. Found: C 48.97, H 3.60, N 14.06%.

2.3.2. Preparation of MCDP via multiple urea linkages

A solution of compound **II** (1.4 g, 0.40 mmol) in anhydrous THF (20 mL) was added into the THF solution of aminized silica gel (4.0 g) under CO_2 atmosphere, and the resulting mixture was kept stirring for 5 min, followed by addition of triphenyl phosphine (2.0 g, 7.62 mmol) in THF solution (20 mL). The reaction was kept under CO_2 at room temperature for 21 h. Then the solvent was removed by filtration and the residue was subjected to the soxhlet extraction with acetone for 24 h.

MCDP: FT-IR (KBr pellet, cm^{-1}): 3445 (NH, str), 1748 (C=O, str), 1604, 1545, 1498 cm^{-1} (arom str), 1096 (O—Si—O, str). Elemental analysis found: C 10.83, H 1.69, N 3.18%. The surface concentration of the β-cyclodextrin derivatives on MCDP: 2.15 × 10^{-2} μmol m^{-2} [25,26]. Total weight loss (from room temperature to 800 °C): 19.76% (Supporting information, Fig. S1).

2.4. Chromatography

MCDP in ACN/IPA was packed into the stainless steel columns (150 mm × 4.6 mm I.D. for analytical column and 250 mm × 10 mm I.D. for semi-preparative column) with Alltech pneumatic HPLC pump (Alltech, USA) by a slurry packing technique, and MeOH was employed as the packing solvent. Using biphenyl as a test sample under the normal-phase mode (hexane/IPA = 90:10, v/v), the obtained HPLC column gave efficiency of 6.4 × 10^4 plates m^{-1}, which was even higher than several commercially available chiral columns [24]. Higher column efficiency would contribute to a better resolution between a pair of enantiomers, with the separation factor unchanged.

Triethylammonium acetate (TEAA) buffer was prepared by using 0.3% triethylamine solution and glacial acetic acid. The pH value of NH_4NO_3 solution was adjusted by adding HNO_3 and $NH_3{\cdot}H_2O$. All mobile phases were filtered through a 0.45 μm membrane prior to use.

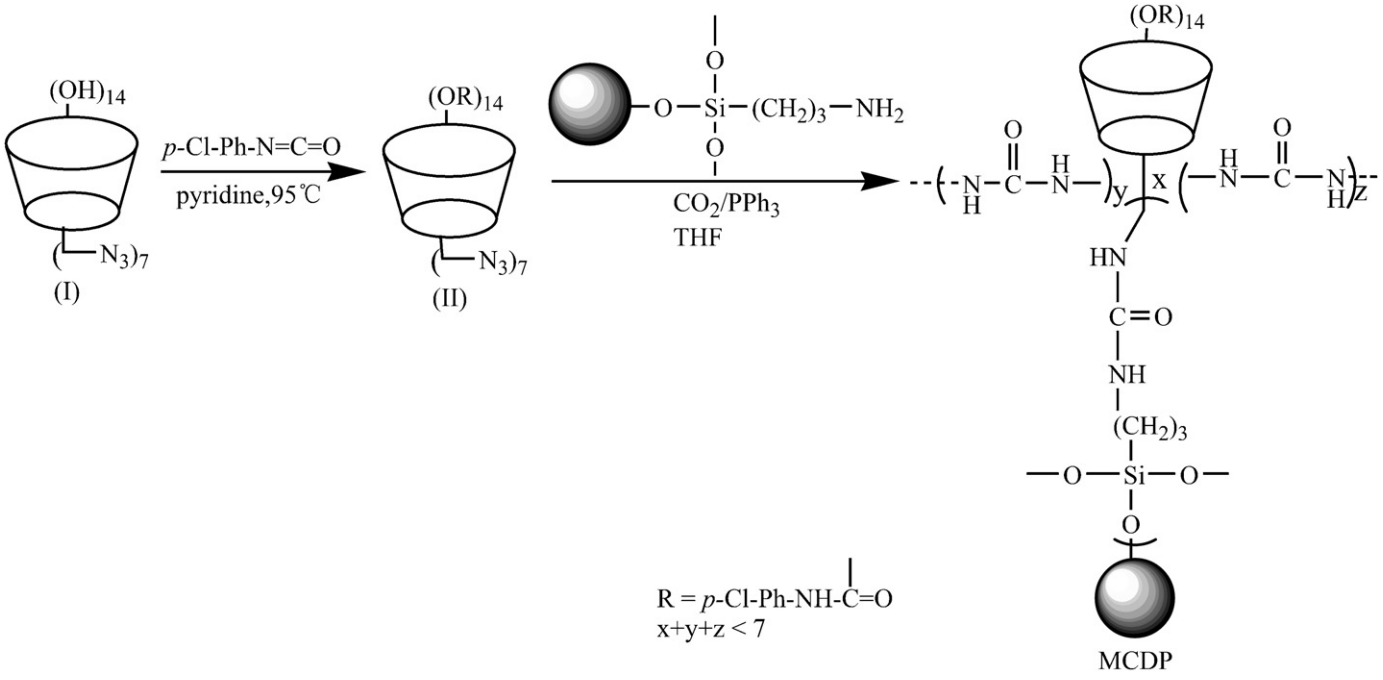

Fig. 2. Synthesis procedure of MCDP.

Complex **1** was dissolved in ethanol at a concentration of 1 mg mL^{-1} and the injected volume was 10 μL for analytical purpose. In semi-preparative separation, the sample concentration was 10 mg mL^{-1} and the injection amount was 1 mg. The flow rates for analytical and semi-preparative resolution were maintained at 1.0 mL min^{-1} and 4.0 mL min^{-1}, respectively. UV detection was carried out at 254 nm. Two pure enantiomers were obtained under the optimum mobile phase (0.05 mol L^{-1} NH_4NO_3/EtOH). Each collected fraction was combined and concentrated by rotary evaporation. Finally, a few samples were dissolved in ethanol for further analyses.

Separation parameters such as retention factor (k), selectivity (α) and the resolution (R_s) for evaluation of enantioseparation were determined using standard formulas on the basis of USP standards [7].

3. Results and discussion

3.1. Preliminary examinations

Resolution of complex **1** on the MCDP column has been investigated in various mobile phases. The results are summarized in Table 1.

In normal-phase mode, complex **1** did not elute from the CSP, owing to the weak elution ability of the hexane/IPA mobile phase. In addition, no separation trends were observed in polar organic phase, such as EtOH, MeOH, ACN, or the mixture without any salt additives. In the normal-phase or polar organic phase, polar solvent molecules occupy the cavity of the cyclodextrin, and chiral analyte molecules could only form weak intermolecular attractions with the derivative moieties located at the rim of the cyclodextrin's cavity.

Modifiers in the mobile phases are noncorrosive and can greatly enhance separation efficiency for cyclodextrin-based CSPs by masking available silanols and other strong adsorption sites [24]. Sometimes, change of additives and pH-value in the mobile phase result in different enantioselectivities and resolutions for chiral compounds. Taking into account that inorganic salts (NaCl, KNO_3, and NH_4NO_3) are fairly insoluble in weak-polar solvents (e.g. hexane), effect of modifiers has been investigated in the polar organic phase (Table 1). Using methanol with different types of salts (TEAA, NaCl, KNO_3 and NH_4NO_3) as mobile phases, moderate retention for **1** (k_1 ranging from 1.88 to 2.82) was achieved on MCDP. The largest R_s value was 0.75 for the mobile phase with NH_4NO_3, and no significant change is observed for the mobile phases with different pH (3.01, 4.27, and 6.80, supporting information, Table S1).

Table 1
Enantioseparation of **1** on the MCDP column under different modes.

Separation mode	k_1	α	R_s	Condition
Normal phase	–[a]	–[a]	–[a]	Hexane/IPA (v/v) = 80/20
Polar organic phase	0.37	1.00	0	MeOH
	1.88	1.10	0.48	0.0400 mol L^{-1} TEAA in MeOH
	1.59	1.10	0.46	0.0125 mol L^{-1} NaCl in MeOH
	2.82	1.10	0.56	0.0125 mol L^{-1} KNO_3 in MeOH
	2.72	1.11	0.75	0.0125 mol L^{-1} NH_4NO_3 in MeOH
Reversed phase	6.20	1.00	0	MeOH/H_2O (v/v) = 80/20
	15.37	1.07	0.25	MeOH/H_2O (v/v) = 75/25
	6.61	1.30	0.53	ACN/H_2O (v/v) = 60/40
	12.65	1.18	0.65	ACN/H_2O (v/v) = 55/45
	9.48	1.11	1.04	MeOH + 0.0500 mol L^{-1} NH_4NO_3:H_2O (v/v) = 90:10
	–[a]	–[a]	–[a]	MeOH/0.3%TEAA (pH 4.0) (v/v) = 70/30

[a] Complex **1** did not elute.

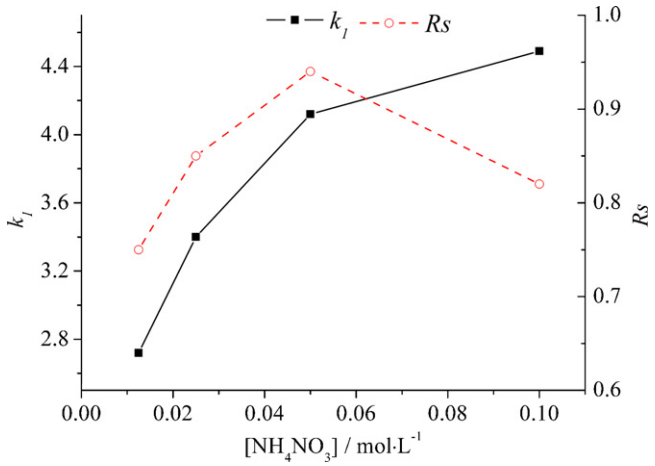

Fig. 3. Effect of salt's concentration on separation of complex **1**. Chromatographic conditions: NH_4NO_3–100% MeOH; pH: 4.27.

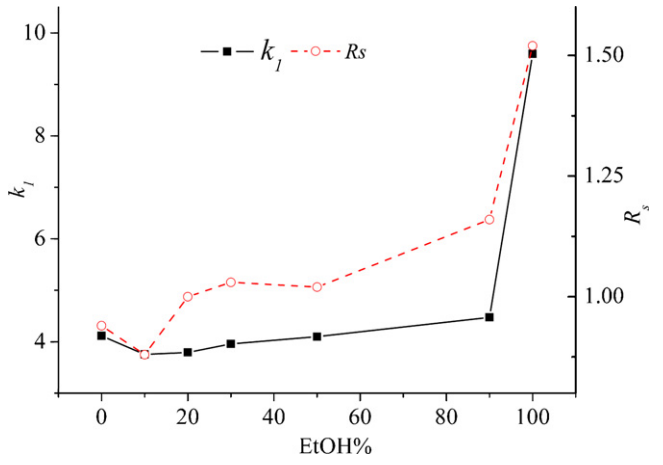

Fig. 4. Effect of ethanol content on separation of complex **1**. Chromatographic conditions: NH_4NO_3 (0.05 mol L^{-1}) in MeOH/EtOH; pH: 4.27.

Compared with polar organic phase, retention factors of complex **1** on the MCDP column greatly increased in the reversed-phase mode (e.g. MeOH/H_2O or ACN/H_2O, Table 1), which might be due to the formation of inclusion complex between hydrophobic cavity of derived β-cyclodextrin and aromatic rings of complex **1** (such as 8-hydroxyquinoline or triphenylphosphine). Furthermore, a slight tendency for separation was observed with H_2O in the mobile phase (α increasing from 1.00 to 1.30). However, because of the large peak width and peak tailing under aqueous conditions, resolution values were very poor (e.g. R_s = 0.53).

While in the reversed-phase mode (e.g. methanol–H_2O) with different types of salts, retention for **1** became much stronger in the column. Although a better separation of complex **1** (R_s = 1.04) was obtained in the mixture of methanol/H_2O (9:1, v/v) with NH_4NO_3 (0.05 mol L^{-1}), it seemed not to be suitable for the further studies. As shown in Fig. S2, several other peaks for impurities appeared, which might be due to unstability of complex **1** in aqueous solution. On the other hand, presence of water in mobile phase would lead to inconvenient post-processing for preparative HPLC. Thus, the polar organic mode with NH_4NO_3 was selected in the continuing work.

3.2. Effect of chromatographic conditions

3.2.1. Effect of NH_4NO_3 concentration

The effect of NH_4NO_3 concentration in the mobile phase has been further investigated for optimization of separation conditions. The retention (k_1) and resolution (R_s) of complex **1** show slightly increasing tendency with the increase of NH_4NO_3 concentration (from 0.0125 to 0.05 mol L^{-1}, Fig. 3). When the concentration of NH_4NO_3 was 0.10 mol L^{-1}, k_1 kept increasing, but R_s was decreased, which might be ascribed to decrease of theoretical plate number in the column from chromatographic peak broadening. Therefore, the optimum concentration of NH_4NO_3 should be 0.05 mol L^{-1} in the mobile phase.

For enantioseparation of basic analytes on crown ether-based chiral stationary phase, Machida et al. put forward two kinds of mechanisms to explain the effect of salt additives: one is competition between analyte molecules and buffer cations that would significantly affect inclusion interactions between analyte and cavity of CSP; another is ion-pair formation between analyte cations and counter anions in mobile phase [27]. When the former interaction is dominant, retention factor decreases with salt's concentration. Otherwise, it would increase. Similar separation mechanisms were proposed on another stationary phase calixarene containing a cavity [28]. In addition, Dai et al. clarified the role of ion pairing in the retention of cation separations in reversed-phase liquid chromatography on the basis of ion-pair formation constants measured by capillary electrophoresis [29,30].

Similar to Chirobiotic V [31], β-cyclodextrin possesses both the cavity and the characteristics of reversed phase. Therefore, separation mechanisms mentioned above could be applied to explain the effect of salt concentration. Increasing trend of k_1 with concentration of NH_4NO_3 supported the description that the ion-pair formation is dominant in our work. Chiral separation may be probably due to electrostatic interaction aroused by the positively charged cations and the negatively charged nitrate-cyclodextrin inclusion complex, as well as π–π interactions resulted from aromatic rings of **1** and *p*-chlorophenyl groups of cyclodextrin-derivatives. In addition, exchange between nitrate anions in the mobile phase and the counter anions (Cl^-) of complex **1** occurs, contributing to formation of $\{Os[CHC(PPh_3)CHC(PPh_3)CH](C_9H_6NO)_2\}^+$–$NO_3^-$–cyclodextrin ion-pairs [16].

3.2.2. Effect of organic modifier

In the follow-up work, other solvents (e.g. EtOH or ACN) were replaced for methanol in the mobile phase. Addition of acetonitrile accelerated the elution of complex **1**, and weakened separation abilities. While the content of ethanol was varied from 0% to 100%, R_s significantly increased from 0.94 to 1.52, as illustrated in Fig. 4. Using ethanol resulted in better separation than methanol. Similar phenomenon was observed in separating two basic analytes on Chirobiotic V column in polar ionic mode [31]. Due to higher polarity, methanol affords stronger solvation to analyte molecules than ethanol, leading to weakening of π–π interactions between analytes and CSP [32]. In addition, methanol molecules have stronger tendency to form hydrogen bonds with —NHCOO— groups on the rim of cyclodetrxin's cavity than ethanol, and occupy active sites favorable for chiral discrimination [33].

3.2.3. Effect of column temperature on enantioseparation

Thermodynamic study is an effective method to investigate chiral recognition mechanism [34,35]. In chromatographic enantioseparation, the relationships between chromatographic data and column temperature are shown as follows:

$$\ln k = -\frac{\Delta H}{RT} + \frac{\Delta S}{R} + \ln \Phi = -\frac{\Delta H}{RT} + \Delta S* \quad (1)$$

$$\ln a = -\frac{\Delta \Delta H}{RT} + \frac{\Delta \Delta S}{R} \quad (2)$$

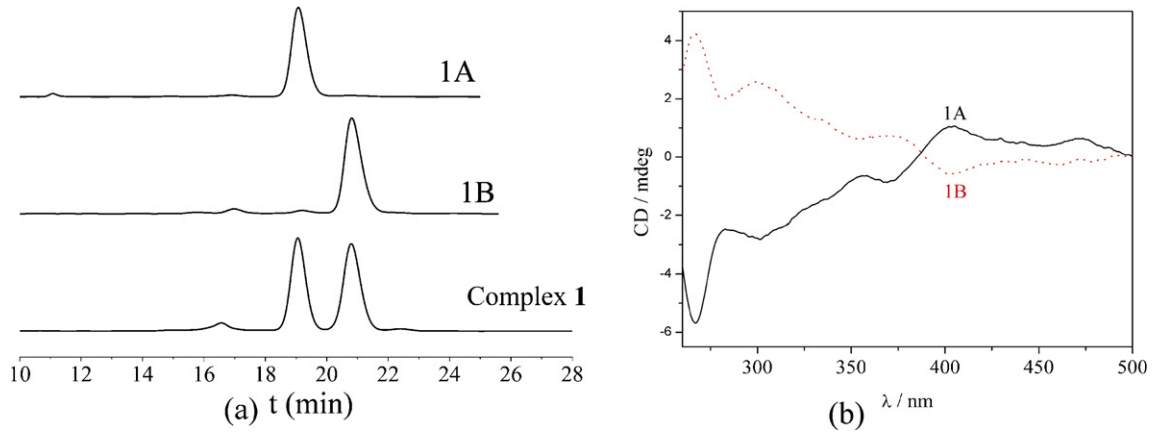

Fig. 5. (a) HPLC chromatograms of two enantiomers, **1**A and **1**B (mobile phase: NH_4NO_3 (0.05 mol L^{-1})–100% EtOH, pH 4.27 and (b) CD spectra of **1**A and **1**B in ethanol solution at room temperature (0.1 cm quartz cuvette, λ in the range from 260 to 500 nm).

where ΔH and ΔS represent the respective changes of enthalpy and entropy when one enantiomer transfers from mobile phase to the stationary phase. $\Delta\Delta H$ and $\Delta\Delta S$ represent the differences of ΔH and ΔS for both enantiomers, respectively. R is the gas constant and Φ the column phase ratio.

The effect of column temperature on enantioseparation of complex **1** has been studied in this work (Table S2). Both the retention factors and resolution gradually decrease with column temperatures from 25 to 45 °C (Fig. S3). A good linear relationship between $\ln k$ vs.$1/T$ was observed ($r^2 > 0.998$, Fig. S4). From the slope and the intercept of the linear $\ln k$ vs.$1/T$ plots, ΔH ($\Delta H_{\mathbf{1A}} = -8.56$ kJ mol^{-1} and $\Delta H_{\mathbf{1B}} = -9.76$ kJ mol^{-1}, **1**A is for the first-eluted enantiomer and **1**B is for the second one) and ΔS^* ($\Delta S^*_{\mathbf{1A}} = -1.19$ J K^{-1} mol^{-1} and $\Delta S^*_{\mathbf{1B}} = -1.58$ J K^{-1} mol^{-1}) are obtained. Moreover, the $\Delta\Delta H$ and $\Delta\Delta S$ values were calculated directly from the differences of ΔH and ΔS^* for the pair of enantiomers, rather than from $\ln\alpha$ vs. $1/T$ plots. Since the values of $\Delta\Delta H$ (-1.20 kJ mol^{-1}) and $\Delta\Delta S$ (-0.39 J K^{-1} mol^{-1}) are negative, enantioseparation of complex **1** could be ascribed to enthalpy-driven process and the increase of temperature would be unfavorable to resolution of **1**. The second-eluted enantiomer forms more stable complex with the selector than the first. Good linear relationship between $\ln k$ vs.$1/T$ also indicates that the conformation of the MCDP, retention and enantioselectivity mechanism have been unchanged in the experimental temperature range [35].

3.3. Comparison of measured and calculated CD spectra

Semi-preparative enantioseparation of complex **1** was carried out on the MCDP column. The chromatographic peaks for the stereoisomers are observed with the similar retention times and their enantiomeric purities reach or exceed 98% (Fig. 5a). The other characterization data were shown in supporting information.

3.3.1. Solution CD spectra of two enantiomers

Circular dichroism spectroscopy is regarded as one of the most useful technique in stereochemistry. The two CD curves of **1**A and **1**B (Fig. 5b and Fig. S5) were measured in ethanol solution at room temperature and look like the mirror images of each other, which indicates that the corresponding compounds must be a pair of enantiomers. In the wavelength range 260–900 nm, complex **1**B shows positive Cotton effects at ca. 266, 298, 371, and 630 nm, and negative Cotton effects at around 404 and 454 nm; while the complex **1**A behaves oppositely at the same wavelengths (see Fig. 5b and Fig. S5)

3.3.2. Theoretical investigation of CD spectra

In order to discriminate the absolute configuration (Δ/Λ) of the compounds based on their observed CD spectra, the ground-state geometry of complex **1** which was assumed as a Λ-type with C_2 symmetry has been optimized using Gaussian03 program package at the DFT/B3LYP level with the mixed basis set: LanL2DZ for the central ion Os^{II}; 6-311G* for the six coordination atoms (including two C, two O and two N atoms) and also for the two P atoms from PPh_3 groups; 6-31G* for 8-hydroxyquinoline anions and the other atoms from osmabenzene ring (including the C atoms directly bound with P atoms); 3-21G* for the H atoms and the other C atoms indirectly linked with P atoms in the PPh_3 ligands [36]. The optimized geometry of complex **1** is illustrated in Fig. S6, some selected bond lengths (Å) and angles (°) are summarized in Table S3. The dihedral angle between osmabenzene plane and 8-hydroxyquinoline anion is 103.03° (measured by their principal axes of inertia), and that of two 8-hydroxyquinoline anions is 138.24°. In addition, the calculated DFT energy levels are displayed in Fig. 6a, and some Kohn–Sham orbitals around HOMO and LUMO are schematically shown in Fig. S7.

Based on the optimized geometry, the excitation energies, oscillator and rotational strengths (both in length and velocity forms) of the first 200 excited states for the complex **1** with Λ-configuration were calculated at the TDDFT/B3LYP level using the same basis set.

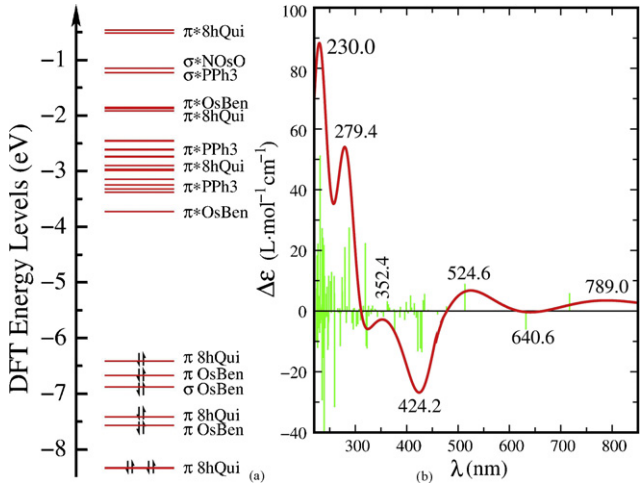

Fig. 6. DFT energy levels (a) and calculated CD spectrum (b) of complex **1** by assuming a Λ configuration. (8hQui for 8-hydroxyquinoline anion, PPh_3 for triphenylphosphine, OsBen for osmabenzene plane without PPh_3 groups, as well as NOsO for Os—N and Os—O bonds.)

Table 2
Selected excitation energies, oscillator and rotational strengths, and assignments for transitions which dominate the CD spectrum.

No.	Sym	λ (nm)	*f*	*R* (DBM)	Assignments[a]
1	*B*	717.06	0.0099	0.5888	$\pi_{8hQui} + \sigma_{OsBen} \rightarrow \pi^*_{OsBen}$
2	*B*	631.95	0.0028	−0.5360	$\sigma_{OsBen} \rightarrow \pi^*_{OsBen}$
3	*A*	513.34	0.0844	0.6422	$\pi_{OsBen+8hQui} \rightarrow \pi^*_{OsBen}$
10	*A*	429.47	0.0348	−0.5050	$\pi_{OsBen+8hQui} \rightarrow \pi^*_{PPh3}, \pi^*_{8hQui}$
11	*B*	426.66	0.0191	−0.4598	$\pi_{8hQui} + \sigma_{NOsO} \rightarrow \pi^*_{OsBen}$
12	*A*	421.60	0.0881	−0.4936	$\pi_{8hQui} + \sigma_{OsBen} \rightarrow \pi^*_{8hQui}, \pi^*_{PPh3}$
55	*A*	322.89	0.0150	−0.4577	$\pi_{8hQui} + \sigma_{NOsO} \rightarrow \pi^*_{8hQui}, \pi^*_{PPh3}$
56	*B*	321.05	0.0162	−0.4294	$\pi_{8hQui} + \sigma_{OsBen} \rightarrow \pi^*_{8hQui}$
57	*A*	319.47	0.0100	0.8345	$\pi_{8hQui} + \sigma_{OsBen} \rightarrow \pi^*_{OsBen+8hQui}$
77	*A*	288.01	0.1101	1.0253	$\sigma_{OsBen} \rightarrow \pi^*_{OsBen+8hQui}$
83	*B*	279.65	0.0299	0.6648	$\sigma_{OsBen+8hQui} \rightarrow \pi^*_{OsBen}$
84	*A*	279.38	0.0173	0.7848	$\pi_{OsBen+8hQui} \rightarrow \pi^*_{PPh3}$
99	*B*	259.72	0.0683	−1.1802	$\pi_{8hQui} + \sigma_{NOsO} \rightarrow \pi^*_{8hQui+OsBen}$
124	*B*	239.12	0.1131	−1.4912	$\sigma_{OsBen+8hQui} \rightarrow \pi^*_{PPh3}, \pi^*_{8hQui}$
125	*A*	238.80	0.0007	0.8087	$\pi_{8hQui} + \sigma_{OsBen} \rightarrow \sigma^*_{8hQui+NOsO}$
144	*B*	231.34	0.0575	1.9115	$\pi_{OsBen+8hQui} \rightarrow \pi^*_{8hQui} + \sigma^*_{NOsO}$

[a] 8hQui for 8-hydroxyquinoline anion, PPh_3 for triphenylphosphine, OsBen for osmabenzene plane without PPh_3 groups, as well as NOsO for Os—N and Os—O bonds.

Parts of the results for transitions which dominate the CD spectrum are listed in Table 2.

By use of the rotational strengths calculated at the TDDFT level, a theoretical CD spectrum (Fig. 6b) was generated as a sum of Gaussians, centered at the calculated wavelengths with integral intensities proportional to the rotational strengths of the corresponding transitions. For transitions with λ < 500 nm, the half band widths at $\Delta\varepsilon_{max}/e$ of the Gaussians were assumed to be proportional to the transition wavelengths with a proportional coefficient 0.085; while for transitions with λ ≥ 500 nm, they were assumed to be 0.4 eV [37–39].

Comparing the calculated and observed CD curves, we see that the two positive CD absorption bands at 230.0 and 279.4 nm in the calculated CD spectrum correspond to those at ca. 266 and 298 nm in the observed one, respectively. In addition, the negative band at 424.2 nm in the theoretical spectrum corresponds to that at ca. 404 nm in the experimental one. A weak band at 352.4 nm in the theoretical spectrum could be ascribed to a shoulder peak at ca. 371 nm in the experimental one, though the peak of the calculated band falls to the negative absorption region due to its intensity being very sensitive to the precision of calculated wavelengths and parameters of half band width. Besides, the calculated CD spectrum also predicts three absorption bands around 524.6, 640.6, and 789.0 nm. Among them, the positive band at 524.6 nm corresponds to that at ca. 630 nm in the measured one (Fig. S5), while the other two CD bands around 640.6 nm and 789.0 nm are too weak to be traced in the observed spectrum due to interfere of noise.

Except for some blue-shift in band wavelengths, the calculated CD spectrum is clearly in good agreement with the observed one as far as the band shape, the sign of major bands, and the relative magnitudes are concerned. Based on this agreement, we conclude that the Os(II) center in the complex **1**B should have Λ-form handedness character. Furthermore, the absorption bands in the experimental CD spectrum could be clearly ascribed: the two positively strong bands at about 266 and 298 nm can be assigned to the $\pi_{OsBen+8hQui} \rightarrow \pi^*_{8hQui} + \sigma^*_{NOsO}$ (or simply denoted as $\pi \rightarrow \pi^*$) and $\sigma_{OsBen} \rightarrow \pi^*_{OsBen+8hQui}$ ($\sigma \rightarrow \pi^*$) transitions, respectively. The negative band at ca. 404 nm is mainly ascribed to the $\pi_{OsBen+8hQui} \rightarrow \pi^*_{8hQui+OsBen+PPh3}$ transition ($\pi \rightarrow \pi^*$). Besides, the rather weak positive band around 630 nm is originated from the $\pi_{OsBen+8hQui} \rightarrow \pi^*_{OsBen}$ transition ($\pi \rightarrow \pi^*$), while the first two transitions with λ > 650 nm are too weak to be observed (Fig. S5).

4. Conclusion

In summary, a new type of β-cyclodextrin-derived chiral stationary phase with multi-urea linkages (MCDP) was synthesized via Staudinger reaction. Enantioseparation and semi-preparation of chiral osmabenzene complex (**1**) have been carried out on the MCDP column by HPLC under polar organic phase, which is the first example for enantioseparation of chiral-only-at-metal osmabenzene complex till now. Effective separation was achieved by the ion-pair formation and electronstatic interaction. Two pure enantiomers of complex **1** are further studied by analytical HPLC, NMR spectra, CD spectra, and theoretical calculations, respectively. The calculated CD spectrum is consistent with the observed result and the absolute configuration of the second elution (**1**B) is Λ-configuration. More detailed studies to investigate the functions and applications toward enantiopure osmabenzene complex (**1**) are being undertaken, such as asymmetric catalysis.

Acknowledgements

Financial supports from Natural Science Foundation of China (Nos. 21171059, 21003053, 20673069, 21273175, 20773098 and 21273139) and Science and Technology Department of Guangdong (Nos. 2010B050300021 and 2011B010400023) are gratefully acknowledged. Many thanks for Professor Hai-ping Xia (Xiamen University, China) to provide the osmabenzene complex in this work.

Appendix A. Supplementary data

Supplementary data associated with this article can be found, in the online version, at http://dx.doi.org/10.1016/j.chroma.2013.01.087.

References

[1] T.J. Ward, K.D. Ward, Anal. Chem. 84 (2012) 626.
[2] T.J. Ward, K.D. Ward, Anal. Chem. 82 (2010) 4712.
[3] Z.B. Zhang, M.H. Wu, R.A. Wu, J. Dong, J.J. Ou, H.F. Zou, Anal. Chem. 83 (2011) 3616.
[4] X.H. Lai, W.H. Tang, S.C. Ng, J. Chromatogr. A 1218 (2011) 3496.
[5] Y.P. Zhang, Z.M. Guo, J.X. Ye, Q. Xu, X.M. Liang, A.W. Lei, J. Chromatogr. A 1191 (2008) 188.
[6] X. Li, Z.M. Zhou, D. Xu, J. Zhang, Talanta 84 (2011) 1080.
[7] Z.B. Zhang, W.G. Zhang, W.J. Luo, J. Fan, J. Chromatogr. A 1213 (2008) 162.
[8] R.Q. Wang, T.T. Ong, S.C. Ng, J. Chromatogr. A 1203 (2008) 185.

[9] L. Chen, L.F. Zhang, C.B. Ching, S.C. Ng, J. Chromatogr. A 950 (2002) 65.
[10] S.C. Ng, T.T. Ong, P. Fu, C.B. Ching, J. Chromatogr. A 968 (2002) 31.
[11] I.W. Muderawan, T.T. Ong, S.C. Ng, J. Sep. Sci. 29 (2006) 1849.
[12] Y. Wang, D.J. Young, T.T.Y. Tan, S.C. Ng, J. Chromatogr. A 1217 (2010) 7878.
[13] Y. Wang, T.T. Ong, L.S. Li, T.T.Y. Tan, S.C. Ng, J. Chromatogr. A 1216 (2009) 2388.
[14] D.W. Armstrong, W. DeMond, B.P. Czech, Anal. Chem. 57 (1985) 481.
[15] L.V. Snegur, V.I. Boev, Y.S. Nekrasov, M.M. Ilyin, V.A. Davankov, Z.A. Starikova, A.I. Yanovsky, A.F. Kolomiets, V.N. Babin, J. Organomet. Chem. 580 (1999) 26.
[16] P. Sun, A. Krishnan, A. Yadav, S. Singh, F.M. MacDonnell, D.W. Armstrong, Inorg. Chem. 46 (2007) 10312.
[17] G.P. Elliott, W.R. Roper, J.M. Waters, J. Chem. Soc. Chem. Commun. (1982) 811.
[18] J.R. Bleeke, Chem. Rev. 101 (2001) 1205.
[19] K.C. Poon, L. Liu, T. Guo, J. Li, H.H.Y. Sung, I.D. Williams, Z. Lin, G. Jia, Angew. Chem. 122 (2010) 2819.
[20] R. Lin, J. Zhao, H.Y. Chen, H. Zhang, H.P. Xia, Chem. Asian J. 7 (2012) 1915.
[21] R. Lin, H. Zhang, S.H. Li, L.Q. Chen, W.G. Zhang, T.B. Wen, H. Zhang, H.P. Xia, Chem. Eur. J. 17 (2011) 2420.
[22] P.R. Ashton, S.E. Boyd, G. Gattuso, E.Y. Hartwell, R. Koniger, N. Spencer, J.F. Stoddart, J. Org. Chem. 60 (1995) 3898.
[23] P.R. Ashton, R. Königer, J.F. Stoddart, J. Org. Chem. 61 (1996) 903.
[24] C.R. Mitchel, D.W. Armstrong, in: G. Gübitz, M.G. Schmid (Eds.), Chiral Separations: Methods and Protocols, Humana Press Inc., Totowa, 2004, p. 61.
[25] A. Berthod, C.D. Chang, D.W. Armstrong, Talanta 40 (1993) 1367.
[26] Q. Qin, S. Zhang, W.G. Zhang, Z.B. Zhang, Y.J. Xiong, Z.Y. Guo, J. Fan, S.R. Zheng, D. Finlow, Y. Yin, J. Sep. Sci. 33 (2010) 2582.
[27] Y. Machida, H. Nishi, K. Nakamura, J. Chromatogr. A 830 (1999) 311.
[28] H. Hashem, T. Jira, J. Chromatogr. A 1133 (2006) 69.
[29] J. Dai, P.W. Carr, J. Chromatogr. A 1072 (2005) 169.
[30] J. Dai, S.D. Mendonsa, M.T. Bowser, C.A. Lucy, P.W. Carr, J. Chromatogr. A 1069 (2005) 225.
[31] H. Hashem, C. Tründelberg, O. Attef, T. Jira, J. Chromatogr. A 1218 (2011) 6727.
[32] Y.Z. Wang, A.X. Wu, Chin. J. Org. Chem. 28 (2008) 997.
[33] C. Lin, W.J. Luo, S. Zhang, W.G. Zhang, S.R. Zheng, J. Fan, W.S. Li, Q. Qin, Z.Y. Guo, J. Sep. Sci. 33 (2010) 1558.
[34] M. Michaud, E. Jourdan, C. Ravelet, A. Villet, A. Ravel, C. Grosset, E. Peyrin, Anal. Chem. 76 (2004) 1015.
[35] B.X. Yao, F.P. Zhan, G.Y. Yu, Z.F. Chen, W.J. Fan, X.P. Zeng, Q.L. Zeng, W. Weng, J. Chromatogr. A 1216 (2009) 5429.
[36] M.J. Frisch, G.W. Trucks, H.B. Schlegel, G.E. Scuseria, M.A. Robb, J.R. Cheeseman, J.A. Montgomery Jr., T. Vreven, K.N. Kudin, J.C. Burant, J.M. Millam, S.S. Iyengar, J. Tomasi, V. Barone, B. Mennucci, M. Cossi, G. Scalmani, N. Rega, G.A. Petersson, H. Nakatsuji, M. Hada, M. Ehara, K. Toyota, R. Fukuda, J. Hasegawa, M. Ishida, T. Nakajima, Y. Honda, O. Kitao, H. Nakai, M. Klene, X. Li, J.E. Knox, H.P. Hratchian, J.B. Cross, V. Bakken, C. Adamo, J. Jaramillo, R. Gomperts, R.E. Stratmann, O. Yazyev, A.J. Austin, R. Cammi, C. Pomelli, J.W. Ochterski, P.Y. Ayala, K. Morokuma, G.A. Voth, P. Salvador, J.J. Dannenberg, V.G. Zakrzewski, S. Dapprich, A.D. Daniels, M.C. Strain, O. Farkas, D.K. Malick, A.D. Rabuck, K. Raghavachari, J.B. Foresman, J.V. Ortiz, Q. Cui, A.G. Baboul, S. Clifford, J. Cioslowski, B.B. Stefanov, G. Liu, A. Liashenko, P. Piskorz, I. Komaromi, R.L. Martin, D.J. Fox, T. Keith, M.A. Al-Laham, C.Y. Peng, A. Nanayakkara, M. Challacombe, P.M.W. Gill, B. Johnson, W. Chen, M.W. Wong, C. Gonzalez, J.A. Pople, Gaussian 03, Revision E.01, Gaussian Inc, Wallingford, CT, 2004.
[37] Y. Wang, Y.K. Wang, J.M. Wang, Y. Liu, Y.T. Yang, J. Am. Chem. Soc. 131 (2009) 8839.
[38] X.L. Su, Y.K. Wang, Y. Wang, J. Jia, X.L. Gao, Acta Phys. Chim. Sin. 27 (2011) 1633.
[39] Y.K. Wang, Application of the Time-Dependent Density Functional Theory to the Study of Chiroptical Properties of Organic and Inorganic Compounds, Shaker Verlag, Aachen, 2003, p. 129.